

Structural Analysis of Protein Interfaces from ^{13}C Direct-Detected Paramagnetic Relaxation Enhancements

Tobias Madl,^{†,‡} Isabella C. Felli,[§] Ivano Bertini,[§] and Michael Sattler^{*,†,‡}

Institute of Structural Biology, Helmholtz Zentrum München, Ingolstädter Landstr. 1, 85764 Neuherberg, Germany, Munich Center for Integrated Protein Science and Chair Biomolecular NMR, Department Chemie, Technische Universität München, Lichtenbergstrasse 4, 85747 Garching, Germany, and Magnetic Resonance Center (CERM), University of Florence, Via L. Sacconi 6, 50019 Sesto Fiorentino, Italy

Received February 26, 2010; E-mail: sattler@helmholtz-muenchen.de

Structure determination of large macromolecular assemblies by solution NMR spectroscopy is challenging and requires optimized biochemical and experimental methods to overcome adverse relaxation properties and spectral overlap, such as optimized pulse sequences,^{1,2} advanced isotope labeling techniques,^{3–5} Residual Dipolar Couplings (RDCs),^{6–8} and spin labeling.^{9–18} Deuterium labeling is required for NMR studies of high molecular weight systems but reduces the number of NOE-derived distance restraints. Additional long-range distance information can be obtained when a paramagnetic group is attached to a protein,^{16,19–21} for example by site-directed nitroxide spin labeling.^{9–11,13,18,22,23} The unpaired electron leads to a distance-dependent paramagnetic relaxation enhancement (PRE), which can be translated into long-range distance restraints for structure calculation.^{9,10,13,15,18,24} Proton (^1H) PREs have a broad range of applications and have been employed for studying the structure, dynamics, and (transient) interactions of biomacromolecules in recent years.^{10–15,18,19,25–27}

Recently, the utility of ^{13}C direct detection for chemical shift assignment²⁸ and structural analysis of high molecular weight systems has been explored.^{26,29–33} For example, direct detection of ^{13}C nuclei in paramagnetic proteins is beneficial due to favorable relaxation properties and enhanced spectral dispersion and has been explored with metal-binding proteins.^{21,27,34–37} When combined with site-directed spin labeling, ^{13}C direct-detected PREs can provide critical information for side chains in domain interfaces, which is difficult to obtain otherwise.

Here, we demonstrate an approach for obtaining long-range distance restraints for structural analysis of perdeuterated proteins and protein complexes by combining site-directed spin-labeling with ^{13}C direct-detected experiments by solution state NMR. This allows PRE measurements for backbone $^{13}\text{C}^\alpha$ and $^{13}\text{C}'$ spins as well as for ^{13}C nuclei of amino acid side chains using ^{13}C detected experiments such as CBCACO ($^{13}\text{C}^\beta$, $^{13}\text{C}^\gamma$ of aspartate/asparagine and glutamate/glutamine; $^{13}\text{C}^\delta$ of glutamate/glutamine) and CON ($^{13}\text{C}^\gamma$ of asparagine, $^{13}\text{C}^\delta$ of glutamine). If fast carbonyl relaxation becomes a limiting factor CC TOCSY and CC NOESY experiments are alternative ^{13}C detected experiments.^{29,30,38} The PREs of these ^{13}C spins provide valuable additional information for side chains in protein binding interfaces, even in perdeuterated proteins. Distance restraints derived from ^{13}C PREs can complement and replace ^1H PREs and thus reduce the number of spin labels required for structural analysis. The approach is particularly suited for studies of large macromolecular assemblies in combination where limited structural information is available due to deuteration.

The presence of fluctuating magnetic fields induced by unpaired electrons leads to enhanced longitudinal and transverse nuclear spin relaxation rates.^{20,39} The PRE is defined as the difference of the relaxation rates of the paramagnetic and diamagnetic states²⁵ and depends on the magnetic properties of the observed nucleus (γ_I), the paramagnetic center, the electron–nucleus distance, and its correlation time (τ_c). In case of an organic radical attached to a macromolecule, such as the nitroxide spin label (long τ_c), transverse ^1H and ^{13}C PREs ($\Gamma_{2,\text{H}}$, $\Gamma_{2,\text{C}}$) are different as they strongly depend on the spectral density at zero frequency, while longitudinal ^1H and ^{13}C PREs ($\Gamma_{1,\text{H}}$, $\Gamma_{1,\text{C}}$) are almost identical for macromolecules tumbling in the spin diffusion limit (Supporting Information). Conformational flexibility of the spin label can be described by an order parameter S^2 and an internal correlation time τ_i of the electron–nucleus distance vector. In general, transverse PREs (Γ_2) are less affected by such internal motion than the longitudinal PREs (Γ_1).⁴⁰ For ^{13}C longitudinal PREs ($\Gamma_{1,\text{C}}$) internal dynamics has a significantly smaller contribution than that for the corresponding proton PREs ($\Gamma_{1,\text{H}}$) (Figure 1; Supporting Information). This is important when distances are derived from the PREs, and it is particularly relevant when analyzing PREs for atoms located in the amino acid side chains, which are typically much more flexible than the backbone. The dependency of the relaxation rates with the correlation time of the internal motion (τ_i) for ^{13}C (Figure 1) shows that internal motion affects longitudinal (Γ_1) ^{13}C PREs much less than the corresponding ^1H PREs and has little effect on transverse (Γ_2) ^{13}C or ^1H PREs. Thus, both ^{13}C Γ_1 and $-\Gamma_2$ can in principle be used to derive distance restraints, even in the presence of internal motion.

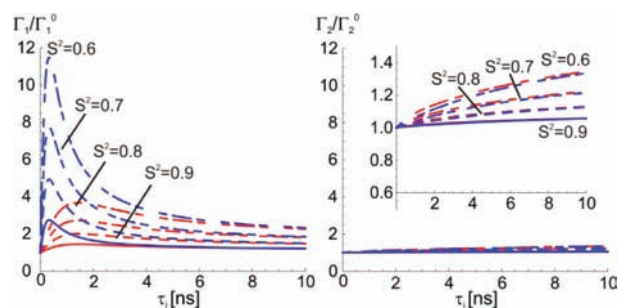


Figure 1. Influence of internal dynamics (τ_i , S^2) on ^1H (blue lines) and ^{13}C PREs (red lines). Γ/Γ^0 is the ratio of the PREs in the presence/absence of internal dynamics. Dotted lines indicate calculations for different values of S^2 assuming $\tau_c = 10$ ns.

We measured $\Gamma_{1,\text{C}}$ and $\Gamma_{2,\text{C}}$ on the tandem RNA Recognition Motif (RRM) domains (RRM1-RRM2) of the splicing factor U2AF65 bound to a polyuridine (U9) RNA oligonucleotide. A

[†] Helmholtz Zentrum München.

[‡] Technische Universität München.

[§] University of Florence.

proxyl nitroxide spin label was conjugated to an engineered cysteine at position 155 in the RRM1 domain. Longitudinal ($^{13}\text{C}^\alpha$, $^{13}\text{C}^\beta$, $^{13}\text{C}'$ Γ_1) and transverse ($^{13}\text{C}'$, Γ_2) PREs were determined from relaxation measurements of the para- and diamagnetic states using ^{13}C direct detected CON and CBCACO experiments^{41–44} (Supporting Information). The ratios of signal intensities in the paramagnetic and diamagnetic states ($I^{\text{para}}/I^{\text{dia}}$)¹⁰ were also determined to estimate transverse PREs (Γ_2). Note that the latter approach is much faster than acquisition of a full set of ^{13}C relaxation data as this requires long interscan recovery delays (Supporting Information). For practical applications we therefore prefer to derive distance restraints from PREs via the experimentally determined $I^{\text{para}}/I^{\text{dia}}$ ratios.

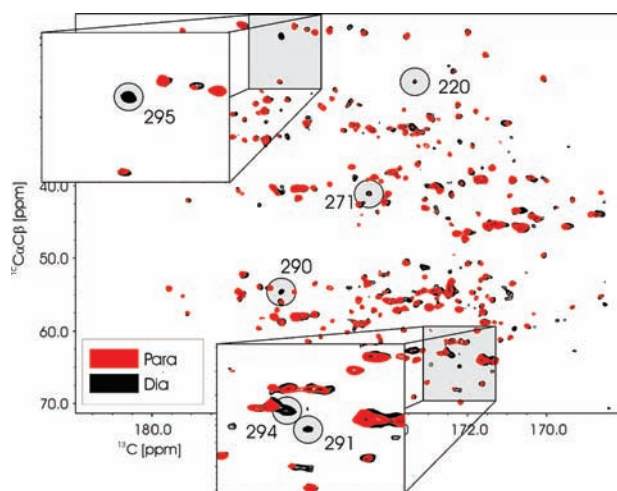


Figure 2. Overlay of CBCACO spectra of $[\text{U}-^2\text{H}, ^{15}\text{N}, ^{13}\text{C}]$ -U2AF65^{148–342, N155C} in complex with U9 RNA in the paramagnetic (red) and diamagnetic state (black). The nitroxide spin label is covalently attached to Cys155. Residues which are close to the spin label and therefore extensively broadened are labeled.

The spin label introduces substantial line broadening resulting from transverse ^{13}C PRE (Γ_2) for many residues in the protein (Figure 2). The observed signal attenuations involve ^{13}C nuclei in the vicinity of the spin label in RRM1 and on a surface patch in RRM2 opposite to the location of the spin label. This shows that the spin label provides information across the RRM1/RRM2 domain interface (Figure 3A). Notably, numerous interdomain PREs are detected for side chain carbons of Asn271 and Asp293 (Figure 3A).

The transverse ^{13}C PREs (Γ_2), derived from experimentally determined signal intensities ($I^{\text{para}}/I^{\text{dia}}$)^{10,18} were converted to distance restraints between the paramagnetic center and the ^{13}C nuclei (Supporting Information). The ^{13}C PRE-derived distance restraints were used together with ^1H PRE-derived distance restraints and residual dipolar coupling data to define the overall arrangement of the two RRM domains of U2AF65 using a protocol that we have recently developed¹⁸ (Supporting Information). In brief, the protocol consists of the following steps: (1) local refinement of the available domain structures of RRM1 and RRM2 using RDC data measured from two alignment media; (2) generation of linker and spin labels and randomization of the linker residues in the RRM1-linker-RRM2 sequence; (3) molecular dynamics simulated annealing restraining RRM1 and RRM2 harmonically to their refined starting structures, with additional dihedral angle restraints from secondary chemical shifts using TALOS,⁴⁵ RDCs, and hydrogen bond restraints. For the quantitative analysis and distance calibration based on intensity ratios ($I^{\text{para}}/I^{\text{dia}}$) it is important to carefully analyze the path of magnetization transfer throughout the pulse sequence. In the case of a $^1\text{H}, ^{15}\text{N}$ HSQC sequence, transverse relaxation of

the amide proton is much stronger than that of the ^{15}N spins, which allows a point-to-point approximation for the electron–nucleus distance. For ^{13}C direct detection spectra such as the CBCACO, the magnetization transfer involves several spins with equal gyromagnetic ratio and, therefore, comparable contributions to the PRE. Therefore, the paramagnetic contributions to transverse relaxation are weighted by the $\langle r^{-6} \rangle$ distance averages of the corresponding spins (e.g., of C^α , C^β , C'). The point-to-point approach breaks down, and ambiguous distance restraints are derived from the ^{13}C Γ_2 PREs and used for the structure calculations.

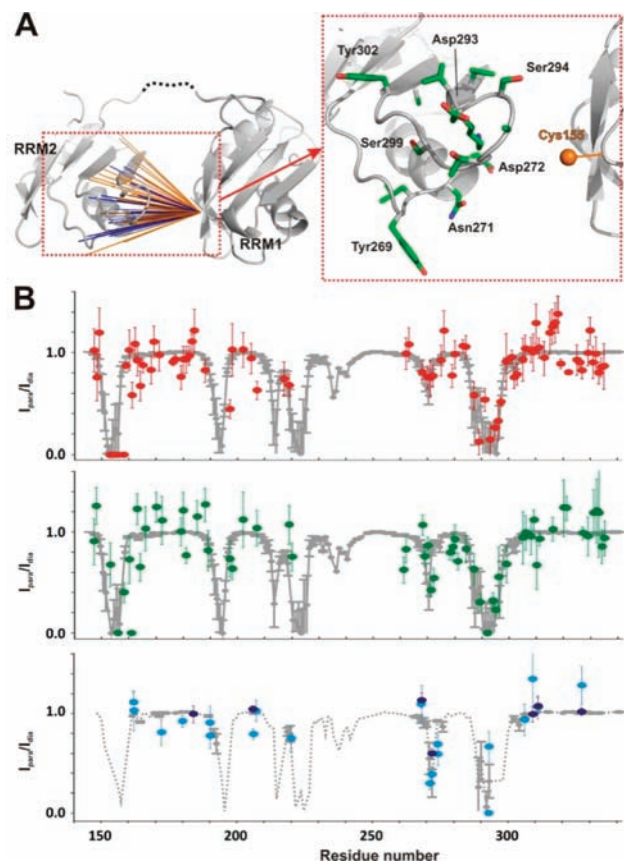


Figure 3. Structural refinement using ^{13}C PRE data. (A) PRE-derived distance restraints are shown in orange (^{13}C) and blue (^1H), respectively. Extensively broadened residues are highlighted. For simplification, the average position of the paramagnetic center is represented as an orange sphere. (B) $^{13}\text{C}^\alpha$, $^{13}\text{C}^\beta$, $^{13}\text{C}'/^{13}\text{C}^\delta$ PRE data included in the structure calculation with error bars indicating the experimental standard deviation. Gray curves and errors are back-calculated PREs for the ensemble of 10 structures. Data points (open symbols) from flexible regions (linker: 228–260, C-terminus: 334–342) are not included in the structure calculation.

The intensity ratios ($I^{\text{para}}/I^{\text{dia}}$) back-calculated from the structures agree well with the experimental data (Figure 3B). The three-dimensional arrangement of the two RRMs resulting from the structure calculation is well-defined by the combination of distance restraints derived from the ^{13}C (158 restraints, from the spin label at residue 155, SL155) and ^1H PREs (946 restraints, from a total of 10 spin labels). Significantly, ^{13}C PREs observed for numerous side chain carbons (i.e., Asn271, Asp293) provide valuable interdomain distance restraints for these charged side chains. This information is not easily available from ^1H detected PRE data (Figure 3) as the corresponding side chains would be deuterated for structural analysis of high molecular weight complexes and no detectable protons are present in terminal carboxyl or carbonyl groups.

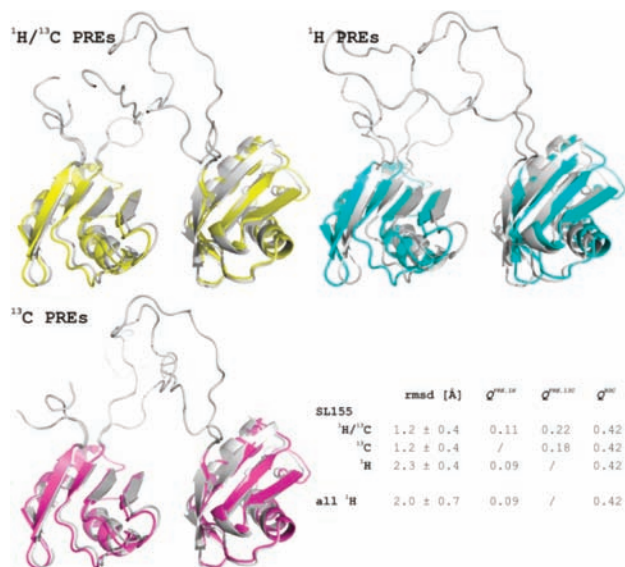


Figure 4. Structure calculations of the RRM12/U9 RNA complex using RDCs and different sets of PRE data for a single spin label at residue 155. For the different calculations the backbone coordinate RMSDs (residues 151–227, 260–334; bundle of the 10 lowest energy structures) to the bundle obtained with all PRE and RDC data, Q^{PRE} (^1H , ^{13}C) and Q^{RDC} , are listed.

Calculations performed with reduced sets of PRE-derived distance restraints demonstrate that structures obtained using all ^1H PREs (i.e., obtained from ten spin labels) are similar to those obtained using only ^{13}C PREs from a single spin label (SL155) (Figure 4). Thus, compared to ^1H PREs carbon detected PREs provide a richer source of restraints that can define protein/domain interfaces equally well with a lower number of spin-labeled samples. Thus, ^{13}C direct-detected PREs provide valuable long-range distance restraints and detailed structural information about domain interfaces. This is especially important for deuterated samples of higher molecular weight complexes where only a few protons are available for the measurement of ^1H PREs.

The approach presented is applicable to proteins and protein–ligand complexes of varying sizes and complexity. The combination of spin labeling and ^{13}C direct detection provides a significantly increased number of restraints per spin label with accordingly higher information content. This results in time saving and improved efficiency for structural analysis of domain interfaces, especially in high molecular weight complexes.

Acknowledgment. T.M. acknowledges support by the EMBO Long Term Fellowship and the Austrian Science Fund (FWF) for a Schrödinger Fellowship. This work was supported by the European Commission, grants 3D Repertoire (LSHG-CT-2005-512028), NIM3 (No. 226507), and EU-NMR (No. 026145).

Supporting Information Available: Details of the theoretical background, methods, and experimental setup and additional data.

This material is available free of charge via the Internet at <http://pubs.acs.org>.

References

- (1) Pervushin, K.; Riek, R.; Wider, G.; Wüthrich, K. *Proc. Natl. Acad. Sci. U.S.A.* **1997**, *94*, 12366.
- (2) Tzakos, A. G.; Grace, C. R. R.; Lukavsky, P. J.; Riek, R. *Annu. Rev. Biophys. Biomol. Struct.* **2006**, *35*, 319.
- (3) Gardner, K. H.; Kay, L. E. *Annu. Rev. Biophys. Biomol. Struct.* **1998**, *27*, 357.
- (4) Tugarinov, V.; Kanelis, V.; Kay, L. E. *Nat. Protoc.* **2006**, *1*, 749.
- (5) Kainosho, M.; Torizawa, T.; Iwashita, Y.; Terauchi, T.; Ono, A. M.; Günter, P. *Nature* **2006**, *440*, 52.
- (6) Tolman, J. R.; Flanagan, J. M.; Kennedy, M. A.; Prestegard, J. H. *Proc. Natl. Acad. Sci. U.S.A.* **1995**, *92*, 9279.
- (7) Tjandra, N.; Bax, A. *Science* **1997**, *278*, 1111.
- (8) Blackledge, M. *Prog. NMR Spectrosc.* **2005**, *46*, 23.
- (9) Gillespie, J. R.; Shortle, D. *J. Mol. Biol.* **1997**, *268*, 170.
- (10) Battiste, J. L.; Wagner, G. *Biochemistry* **2000**, *39*, 5355.
- (11) Gaponenko, V.; Howarth, J. W.; Columbus, L.; Gasmi-Seabrook, G.; Yuan, J.; Hubbell, W. L.; Rosevear, P. R. *Protein Sci.* **2000**, *9*, 302.
- (12) Iwahara, J.; Clore, G. M. *Nature* **2006**, *440*, 1227.
- (13) Liang, B.; Bushweller, J. H.; Tamm, L. K. *J. Am. Chem. Soc.* **2006**, *128*, 4389.
- (14) Tang, C.; Iwahara, J.; Clore, G. M. *Nature* **2006**, *444*, 383.
- (15) Volkov, A. N.; Worrall, J. A.; Holtzmann, E.; Ubbink, M. *Proc. Natl. Acad. Sci. U.S.A.* **2006**, *103*, 18945.
- (16) Otting, G. *J. Biomol. NMR* **2008**, *42*, 1.
- (17) Bermejo, G. A.; Strub, M. P.; Ho, C.; Tjandra, N. *J. Am. Chem. Soc.* **2009**, *131*, 9532.
- (18) Simon, B.; Madl, T.; Mackereth, C. D.; Nilges, M.; Sattler, M. *Angew. Chem., Int. Ed.* **2010**, *49*, 1967.
- (19) Bertini, I.; Luchinat, C.; Rosato, A. *Prog. Biophys. Mol. Biol.* **1996**, *66*, 43.
- (20) Bertini, I.; Luchinat, C.; Parigi, G. *Solution NMR of Paramagnetic Molecules*; Elsevier: 2001.
- (21) Bertini, I.; Luchinat, C.; Parigi, G.; Pierattelli, R. *ChemBioChem* **2005**, *6*, 1536.
- (22) Hubbell, W. L.; Altenbach, C. *Curr. Opin. Struct. Biol.* **1994**, *4*, 566.
- (23) Iwahara, J.; Anderson, D. E.; Murphy, E. C.; Clore, G. M. *J. Am. Chem. Soc.* **2003**, *125*, 6634.
- (24) Kosen, P. A. *Methods Enzymol.* **1989**, *177*, 86.
- (25) Clore, G. M.; Iwahara, J. *Chem. Rev.* **2009**, *109*, 4108.
- (26) Madl, T.; Bermel, W.; Zangger, K. *Angew. Chem., Int. Ed.* **2009**, *48*, 8259.
- (27) Machonkin, T. E.; Westler, W. M.; Markley, J. L. *J. Am. Chem. Soc.* **2004**, *126*, 5413.
- (28) Bermel, W.; Bertini, I.; Felli, I. C.; Piccioli, M.; Pierattelli, R. *Prog. Nucl. Magn. Reson. Spectrosc.* **2006**, *48*, 25.
- (29) Eletsky, A.; Moreira, O.; Kovacs, H.; Pervushin, K. *J. Biomol. NMR* **2003**, *26*, 167.
- (30) Bertini, I.; Felli, I. C.; Kummerle, R.; Moskau, D.; Pierattelli, R. *J. Am. Chem. Soc.* **2004**, *126*, 464.
- (31) Shimba, N.; Kovacs, H.; Stern, A. S.; Nomura, A. M.; Shimada, I.; Hoch, J. C.; Craik, C. S.; Dotsch, V. *J. Biomol. NMR* **2004**, *30*, 175.
- (32) Takeuchi, K.; Sun, Z. Y. J.; Wagner, G. *J. Am. Chem. Soc.* **2008**, *130*, 17210.
- (33) Matzapetakis, M.; Turano, P.; Theil, E. C.; Bertini, I. *J. Biomol. NMR* **2007**, *38*, 237.
- (34) Bermel, W.; Bertini, I.; Felli, I. C.; Kummerle, R.; Pierattelli, R. *J. Am. Chem. Soc.* **2003**, *125*, 16423.
- (35) Machonkin, T. E.; Westler, W. M.; Markley, J. L. *J. Am. Chem. Soc.* **2002**, *124*, 3204.
- (36) Bertini, I.; Felli, I. C.; Luchinat, C.; Parigi, G.; Pierattelli, R. *ChemBioChem* **2007**, *8*, 1422.
- (37) Kostic, M.; Pochapsky, S. S.; Pochapsky, T. C. *J. Am. Chem. Soc.* **2002**, *124*, 9054.
- (38) Fischer, M. W. F.; Zeng, L.; Züderweg, E. R. P. *J. Am. Chem. Soc.* **1996**, *118*, 12457.
- (39) Abragam, A. *Principles of Nuclear Magnetism*; Oxford University Press: Oxford, 1961.
- (40) Iwahara, J.; Schwieters, C. D.; Clore, G. M. *J. Am. Chem. Soc.* **2004**, *126*, 5879.
- (41) Bermel, W.; Bertini, I.; Duma, L.; Felli, I. C.; Emsley, L.; Pierattelli, R.; Vasos, P. R. *Angew. Chem., Int. Ed.* **2005**, *44*, 3089.
- (42) Bermel, W.; Bertini, I.; Felli, I. C.; Kummerle, R.; Pierattelli, R. *J. Magn. Reson.* **2006**, *178*, 56.
- (43) Arnesano, F.; Banci, L.; Bertini, I.; Felli, I. C.; Luchinat, C.; Thompsett, A. R. *J. Am. Chem. Soc.* **2003**, *125*, 7200.
- (44) Bermel, W.; Bertini, I.; Felli, I. C.; Peruzzini, R.; Pierattelli, R. *ChemPhysChem* **2010**, *11*, 689.
- (45) Cornilescu, G.; Delaglio, F.; Bax, A. *J. Biomol. NMR* **1999**, *13*, 289.

JA1014508